News & Views Open Access

Innovative 2D heterostructure nanocavity for robust single-soliton mode-locking

Haiyi Liu[1,2], Hai Liu[1,2], Fang Wang[1,2], Pengfei Qi[1,2,3,*], Lie Lin[1,2] and Weiwei Liu[1,2]

Abstract

A robust saturable absorber that integrates MoS_2-BN-graphene-BN-MoS_2 nanocavity on fibre is proposed and demonstrated. The proposed absorber lowers saturation intensity to 22 MW cm^{-2}, raises polarisation tolerance to 85%, and stabilises single-soliton mode-locking in all-fibre lasers. This work provides a practical and high-performance solution for achieving stable mode-locking in all-fibre lasers, effectively overcoming the inherent limitations of conventional 2D saturable absorbers.

Keywords: Satuable absorber, 2D material, Mode-locking

Ultrafast lasers delivering femtosecond pulses with high peak power have become one of the most effective tools in ultraprecision manufacturing, strong-field physics, nonlinear optics, medical diagnosis, astronomical detection, precision measurement, and fundamental research[1–3]. Among these, the passively mode-locked ultrafast fibre laser (MLFL) based on a saturable absorber (SA) is one of the most convenient routes for developing pulses shorter than 100 fs, thereby offering high beam quality, low cost, efficient cavity, alignment-free compact design, and excellent compatibility[3–5].

Progress in SA design has followed the development of materials that show saturable absorption. For many years, the dominant SA has been the semiconductor saturable absorber mirror (SESAM), a quantum-well structure grown using molecular beam epitaxy (MBE)[6,7]. The high stability of SESAM makes it a reliable choice. However, SESAMs suffer from picosecond recovery, a narrow working band, low damage threshold, complex fabrication, and high costs. Thus, the community has been constantly searching for substitutes with faster recovery times and broader spectral ranges[8,9].

Emerging low-dimensional (LD) materials with various advantages over SESAM provide a new prospect for the development of pulsed fibre lasers because of their distinct structures and physical properties[10,11]. Pauli-blocking instantaneously reduces absorption when the lower energy level is depleted[10,12], producing regular femtosecond pulse trains[12]. These LD SAs offer broader operating spectra than SESAMs, thus providing a clear path to the next generation of low-threshold, low-cost MLFLs[13]. Among LD materials, graphene is particularly promising because of its ultrafast recovery time (< 100 fs) and linear energy dispersion. Graphene enables mode locking without disturbing the optical mode across a broad spectral range (from visible to infrared) with ultrashort pulses (< 90 fs) and high repetition rates (> 9 GHz)[14,15]. However, unstable output states and background pulses prior to soliton formation restrict its practical utilisation[16].

To address the aforementioned challenges, Shao *et al.*[17] constructed a nanocavity SA by transferring a MoS_2-BN-graphene-BN-MoS_2 heterostructure onto the end facet of a single-mode fibre (Fig. 1a). The refractive-index contrast

Correspondence: Pengfei Qi (qipengfei@nankai.edu.cn)
[1]Institute of Modern Optics, Eye Institute, Nankai University, Tianjin 300350, China
[2]Tianjin Key Laboratory of Micro-scale Optical Information Science and Technology, Tianjin 300350, China
Full list of author information is available at the end of the article.

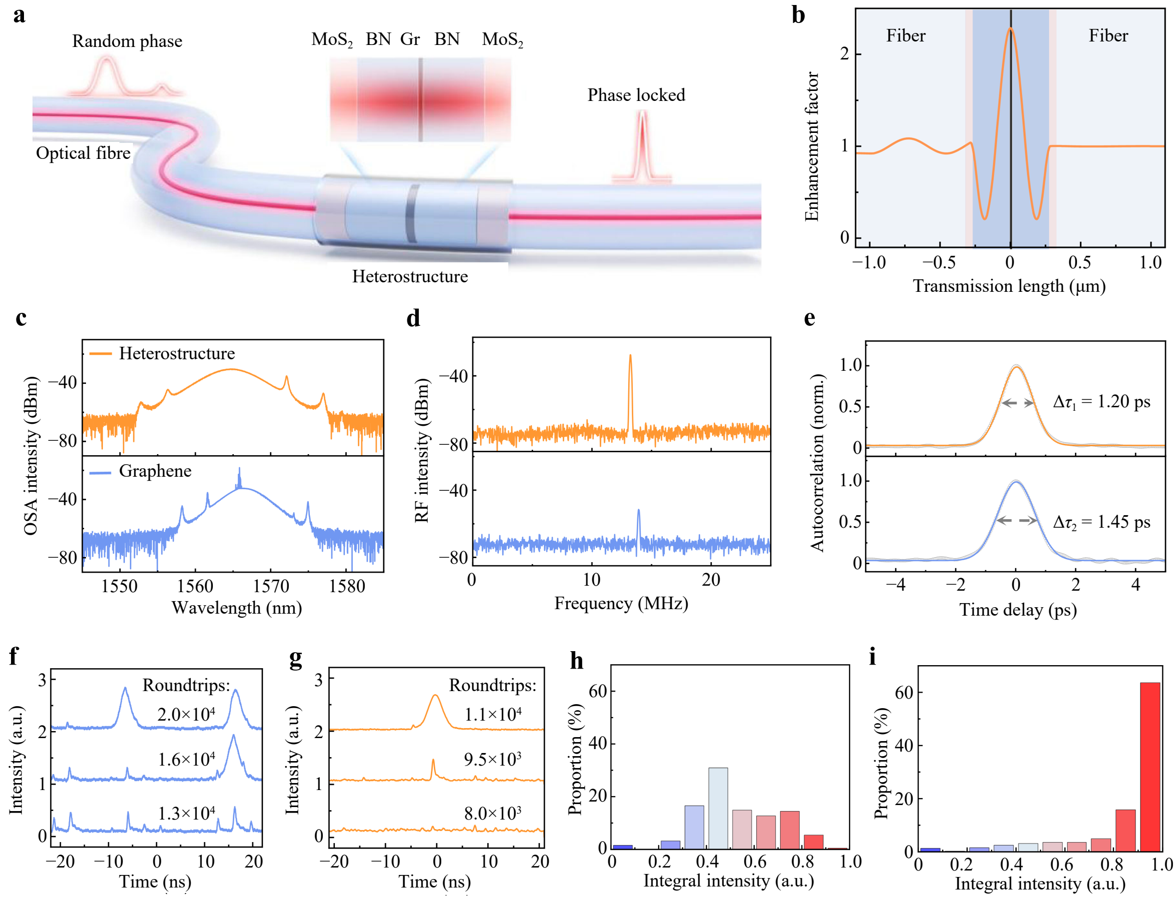

Fig. 1 a Schematic representation of the MoS_2-BN-graphene-BN-MoS_2 heterostructure embedded between optical fibre end facets. **b** Internal optical field intensity distribution of the heterostructure. Optical field intensity in graphene can be enhanced by ~230% with a BN thickness of 240 nm. **c** Spectra of output lasers with bare graphene-SA and heterostructure-SA. **d** RF spectra measured for bare graphene-SA and heterostructure-SA. **e** Autocorrelation trace with FWHM of ~1.20 ps for heterostructure-SA and ~1.45 ps for graphene-SA. **f-g** Temporal profiles at representative roundtrips during pulse formation obtained with **f** graphene-SA and **g** heterostructure-SA. **h-i** Statistics on the integral intensities of **h** graphene-SA and **i** heterostructure-SA.

between MoS_2 and BN formed a nanocavity. Within this nanocavity, the optical field intensity in the graphene layer was enhanced by 230% owing to the standing-wave effect (Fig. 1b), and the fitted saturation intensity dropped from 62.9 MW cm^{-2} for bare graphene to 22.0 MW cm^{-2}. Consequently, the heterostructure enabled stable single-soliton mode-locking and significantly improved polarisation tolerance.

The heterostructure was inserted into an all-fibre ring cavity pumped at 980 nm. The output spectrum shows a conventional soliton with clear Kelly sidebands; the non-soliton component that appears at 1565.8 nm with bare graphene is clearly removed (Fig. 1c). The radio-frequency signal exhibits a signal-to-noise ratio of 45 dB, compared with 22 dB for bare graphene (Fig. 1d); the pulse duration of 1.45 is reduced to 1.20 ps (Fig. 1e); and the output power has increased to 92.5 mW without any damage.

Real-time time-stretch dispersive Fourier transform measurements were used to resolve the soliton build-up process. With bare graphene, the laser passed through relaxation oscillation and energy fluctuation, reaches 11% in Fig. 1f, and a second soliton appears after approximately 20,000 rounds. With this heterostructure, the process stops at the single-pulse stage, and a stable soliton with only 3% energy fluctuation is established after approximately 11,000 round trips, with no splitting observed (Fig. 1g).

Polarisation tolerance was examined using an automatic controller that covered the entire Poincaré sphere. Without the SA, the cavity produced only continuous-wave light. With bare graphene, single-pulse mode-locking was obtained for 20% of the polarisation states (Fig. 1h). With the heterostructure, the single-pulse state is preserved for

85% of the states and pulse splitting is almost eliminated (Fig. 1i). The saturable absorption-related self-amplitude modulation coefficient increased from 6.7×10^{-4} to 2.3×10^{-3}, far exceeding the mode-locking threshold and consequently dramatically improving the polarisation tolerance.

In summary, the developed 2D heterostructure nanocavity demonstrates strong compatibility for integration onto optical fibre end facets, showing significant promise for enhancing the performance and enabling the miniaturisation of all-fibre devices. This study not only provides a competitive alternative to traditional SESAMs by overcoming their inherent limitations such as narrow bandwidth and complex fabrication, but also effectively addresses the instability and polarisation sensitivity issues commonly associated with simple LD material-based SAs. Further optimisation of the heterojunction design and cavity dispersion management may extend the capability of the platform to support multiwavelength mode-locking and optical frequency comb production, highlighting its utility in communication, high-accuracy sensing, and biomedical photonic applications.

Author details

[1]Institute of Modern Optics, Eye Institute, Nankai University, Tianjin 300350, China. [2]Tianjin Key Laboratory of Micro-scale Optical Information Science and Technology, Tianjin 300350, China. [3]Academy for Advanced Interdisciplinary Studies, Nankai University, Tianjin 300071, China

Data availability

All data are available from the corresponding authors upon reasonable request.

Conflict of interest

The authors declare no conflicts of interest.

Received: 17 September 2025 Revised: 04 November 2025 Accepted: 06 November 2025

Published online: 10 December 2025

References

1. Chou, S. Y., Keimel, C. & Gu, J. Ultrafast and direct imprint of nanostructures in silicon. *Nature* **417**, 835-837 (2002).
2. Marcinkevičius, A. et al. Femtosecond laser-assisted three-dimensional microfabrication in silica. *Optics Letters* **26**, 277-279 (2001).
3. Keller, U. Recent developments in compact ultrafast lasers. *Nature* **424**, 831-838 (2003).
4. Fermann, M. E. & Hartl, I. Ultrafast fibre lasers. *Nature Photonics* **7**, 868-874 (2013).
5. Guo, B. et al. 2D layered materials: synthesis, nonlinear optical properties, and device applications. *Laser & Photonics Reviews* **13**, 1800327 (2019).
6. Wei, C. et al. 34 nm-wavelength-tunable picosecond Ho^{3+}/Pr^{3+}-codoped ZBLAN fiber laser. *Optics Express* **25**, 19170-19178 (2017).
7. Gluth, A. et al. GaSb-based SESAM mode-locked Tm: YAG ceramic laser at 2 μm. *Optics Express* **23**, 1361-1369 (2015).
8. Wang, J. L. et al. Recent advances in mode-locked fiber lasers based on two-dimensional materials. *Nanophotonics* **9**, 2315-2340 (2020).
9. Zhang, Y. N. et al. Advances and challenges of ultrafast fiber lasers in 2-4 μm mid-infrared spectral regions. *Laser & Photonics Reviews* **18**, 2300786 (2024).
10. Di Gaspare, A. et al. Electrically tunable nonlinearity at 3.2 terahertz in single-layer graphene. *ACS Photonics* **10**, 3171-3180 (2023).
11. Yamashita, S. et al. Saturable absorbers incorporating carbon nanotubes directly synthesized onto substrates and fibers and their application to mode-locked fiber lasers. *Optics Letters* **29**, 1581-1583 (2004).
12. Bao, Q. L. et al. Atomic-layer graphene as a saturable absorber for ultrafast pulsed lasers. *Advanced Functional Materials* **19**, 3077-3083 (2009).
13. Sun, Z. P. et al. Graphene mode-locked ultrafast laser. *ACS Nano* **4**, 803-810 (2010).
14. Bonaccorso, F. et al. Graphene photonics and optoelectronics. *Nature Photonics* **4**, 611-622 (2010).
15. Brida, D. et al. Ultrafast collinear scattering and carrier multiplication in graphene. *Nature Communications* **4**, 1987 (2013).
16. Han, M. M. et al. Polarization dynamic patterns of vector solitons in a graphene mode-locked fiber laser. *Optics Express* **23**, 2424-2435 (2015).
17. Shao, J. H. et al. Robust mode-locking in all-fiber ultrafast laser by nanocavity of two-dimensional heterostructure. *Light: Science & Applications* **14**, 301 (2025).